A peer-reviewed version of this preprint was published in PeerJ on 15 December 2020.

New insights into the mechanism of Schiff base synthesis from aromatic amines in the absence of acid catalyst or polar solvents

Pedro J Silva [Corresp. 1]

[1] FP-ENAS/Fac. de Ciências da Saúde, Universidade Fernando Pessoa, Porto, Portugal

Corresponding Author: Pedro J Silva
Email address: pedros@ufp.edu.pt

Extensive computational studies of the imine synthesis from amines and aldehydes in water have shown that the large-scale structure of water is needed to afford appropriate charge delocalisation and enable sufficient transition state stabilisation. These insights cannot, however, be applied to the understanding of the reaction pathway in apolar solvents due their inability to form extensive hidrogen-bonding networks. In this work, we perform the first computational studies of this reaction in apolar conditions. This density-functional study of the reaction of benzaldehyde with four closely related aromatic amines (aniline, *o*-toluidine, *m*-toluidine and *p*-toluidine) shows that an additional molecule of amine may provide enough stabilization of the first transition state even in the absence of a hydrogen bonding network. Our computations also show that the second reaction step cannot take place unless an extra proton is added to the system but, crucially, that reaction rate is so high that even picomolar amounts of protonated base are enough to achieve realistic rates. Additional computations show that those minute amounts of protonated base may be obtained under reaction conditions without the addition of extraneous acid through the auto-protolysis of the amines themselves. To our knowledge, this is the first report of a role for the auto-protolysis of anilines in their extensive reactional repertoire.

1 Introduction

2

3 Imines can be readily synthesized through the reversible reaction of amines with aldehydes. This
4 reaction proceeds through an addition step which forms a carbinolamine intermediate, which is
5 then dehydrated to the imine in the rate-determining step. The released water is usually removed
6 from the system to shift the equilibrium towards the products. The reaction rate is quite sensitive
7 to pH: moderate amounts of acid greatly accelerate it(Santerre, Hansrote & Crowell, 1958), but
8 excess acid prevents it(Jencks, 1959 and references therein). The decrease in reaction rate at very
9 low pH is due to the protonation of the amine, which renders it unable to directly attack the
10 carbonyl, whereas protonation of the carbinolamine is required to achieve high rates of
11 dehydration(Jencks, 1964) (Figure 1). Acid catalysis has also been postulated to proceed through
12 protonation of the carbonyl group, rendering it more susceptible to nucleophilic attack by the
13 amine(Hammett, 1940). The reaction may also take place in the absence of acid catalysis(Law,
14 1912; Campbell et al., 1948; Crowell & Peck, 1953), especially with primary amines.
15 Computational studies of this reaction have shown that in the absence of charge stabilization by
16 solvent the activation energies of the formation of the carbinolamine (Hall & Smith, 1998;
17 Ding, Cui & Li, 2015; Ćmikiewicz, Gordon & Berski, 2018) are prohibitively high (above 25
18 kcal·mol^{-1}) and the activation energies of its dehydration to imine (Hall & Smith, 1998;
19 Ćmikiewicz, Gordon & Berski, 2018) are even higher (between 45 and 55 kcal·mol^{-1}).
20 Incorporation of one(Hall & Smith, 1998; Ding, Cui & Li, 2015) or two(Hall & Smith, 1998)
21 water molecules as proton transfer assistants greatly facilitates the formation of the
22 carbinolamine by decreasing the activation energy to 8-16 kcal·mol^{-1} but still affords large
23 barriers incompatible with room-temperature reaction (26.7 kcal·mol^{-1}) for the dehydration
24 step(Hall & Smith, 1998). Realistic barriers are, however, obtained when a large number of
25 explicit water molecules (from 9 to 29) are included in the model(Solís-Calero et al., 2012),
26 enabling extensive stabilization of the nascent charges present in the transition state of the
27 dehydration step. Since so far all the computational work on this reaction has been performed on
28 systems including only water as solvent, the aforementioned insights cannot be directly applied
29 to reactions in apolar or aprotic solvents, such as the condensation of benzaldehyde with aniline
30 (or toluidines), which is experimentally observed to proceed readily and exothermically in the

31   absence of an acid catalyst(Law, 1912; Campbell et al., 1948; Crowell & Peck, 1953) or

32   additional solvent. The present manuscript fills this gap by describing the first computational

33   study of this reaction in the presence of explicit non-aqueous solvent molecules.

34   **Computational methods**

35   The reaction mechanism was investigated using the widely used PBE0 functional(Adamo &

36   Barone, 1999). All geometry optimizations were performed with the Firefly(Granovsky)

37   quantum chemistry package, which is partially based on the GAMESS (US)(Schmidt et al.,

38   1993) code, using autogenerated delocalized coordinates(Baker, Kessi & Delley, 1996). In

39   geometry optimizations, the aug-pcseg-0 basis set(Jensen, 2014) was used for heavy atoms and

40   the pcseg-0 basis set was used for hydrogen. Zero-point and thermal effects on the free energies

41   at 298.15 K were computed at the optimized geometries. DFT energies of the optimized

42   geometries obtained with each density functional were then computed using the aug-pcseg-2 (for

43   heavy atoms) and pcseg-2 basis sets (for hydrogen atoms)(Jensen, 2014), which are expected to

44   be close to the complete basis set limit for DFT. Auto-protolysis constants (pKs) of aniline,

45   toluidines, acetonitrile, and nitromethane, were computed by comparing the energies of

46   separately optimized neutral clusters of each molecule to clusters of the same size which

47   included one single instance of protonated (or deprotonated) molecule. In all cases, intra- and

48   inter-molecular dispersion effects were included in the geometry optimization, frequency

49   calculation, and high-level single point steps using the DFT-D3 formalism developed by Grimme

50   et al. (Grimme et al., 2010). Solvation effects in tetrahydrofuran and aniline were computed

51   using the Polarizable Continuum Model(Tomasi & Persico, 1994; Mennucci & Tomasi, 1997;

52   Cossi et al., 1998) implemented in Firefly. Dispersion and repulsion interactions with the

53   continuum solvent were computed using the method developed by Amovili and

54   Mennucci(Amovilli & Mennucci, 1997).

55

56   **Results**

57   The reactions of benzaldehyde with aniline and its three mono-methylated derivatives (*o*-

58   toluidine, *m*-toluidine, and *p*–toluidine) were studied in the gas phase. In all cases, the

59   most stable initial arrangement of aldehyde and the aromatic amine finds both molecules

60   parallel to each other due to the interaction between their aromatic clouds (Figure 2).

61   Formation of these pre-reactional complexes from the previously separated molecules

62   entails a loss of entropy between 11 and 11.8 kcal·mol^{-1} and is therefore mildly

63   endergonic, by 5.3 to 8.2 kcal·mol^{-1} (Table 1). Subsequent formation of the carbinolamine

64   intermediate may proceed through simultaneous attack of the carbonyl carbon atom by

65   the amine lone pair and proton transfer from the amine to the carbonyl oxygen atom. The

66   geometry of this transition state (Figure 2) is virtually identical for the four aromatic

67   amines studied, with a N–C distance of 1.643–1.650 Å, a NH–O distance of 1.425–1.439

68   Å and a C-O distance very close to that of a C-O single bond. The transition states are,

69   however, very hard to reach as they lie 27–29 kcal·mol^{-1} above the pre-reactional

70   complex state and 33.5–36.9 kcal·mol^{-1} above the infinitely separated reactants (Table 1).

71   Since these high activation energies are incompatible with the experimentally observed

72   syntheses of imines from aldehyde and aromatic amines at temperatures between 0 and 60

73   ºC (Allen & VanAllan, 1941; Campbell et al., 1948; Crowell & Peck, 1953), the actual

74   reaction mechanism must be more complex than commonly postulated.

75   Additional computations showed that the inclusion of an additional molecule of amine greatly

76   facilitates the formation of the carbinolamine by assisting the proton transfer from the amine to

77   the carbonyl oxygen (Figure 3A), which allows the partial negative charge on the oxygen to

78   become more efficiently stabilized (-0.35 instead of the original -0.43). The increased energetic

79   stabilization more than offsets the larger entropic penalty due to the presence of three (rather

80   than two) molecules in the pre-reactional complex, yielding barriers of 12.8–14.1 kcal·mol^{-1}

81   above the pre-reactional complex state and 19.1–24.8 kcal·mol^{-1} above the infinitely separated

82   reactants (Table 2). The overall exergonicity of the reaction (vs. pre-reactional complex) is

83   decreased by 3–7 kcal·mol^{-1} with the inclusion of the additional molecule of base. Interestingly,

84   the higher barriers (above the pre-reactional complex) are observed for the *o*- and *p*-toluidines,

85   whereas the barrier for *m*-toluidine is virtually indistinguishable from that of aniline, which is

86   opposite to the trend observed in the absence of the additional molecule of amine.

87   Carbinolamine dehydration proved to be difficult (Table 2), with barriers ranging between 27

88   and 32.2 kcal·mol^{-1} relative to the carbinolamine. Previous computational studies of this reaction

89   (Hall & Smith, 1998; Solís-Calero et al., 2012) showed that this step is also difficult in water

90   models, unless large solvent cages are used, which allow very efficient charge delocalization

91   throughout the hydrogen-bonded network (Solís-Calero et al., 2012). Since such stabilization is

92   exceedingly unlikely to be available in aromatic amine solvents due to their inability to form

93   such extended networks, other possibilities of achieving acceptable reaction rates for the

94   dehydration step were analysed. Inspired by the observation of dimeric derivatives of imines

95   obtained through electrochemical reduction (Law, 1912) we first evaluated the feasibility of

96   stabilizing the carbinolamine dehydration step with a second molecule of carbinolamine. The

97   barriers obtained for this mechanism again lie too high, from 28.5 to 30.5 kcal·mol^{-1}, effectively

98   ruling out this possibility in spite of the mutually-stabilizing influences of one carbinolamine

99   molecule on the other (Figure 4). These results strongly suggest that attempts to stabilize the

100 transition states exclusively through hydrogen bonding towards the leaving hydroxyl group

101 (Figure 3C) or its protonation by neutral functional groups (Figure 4) are not likely to be

102 successful.

103 In contrast, addition of one protonated molecule of amine strongly facilitates the dehydration

104 step since the extra proton provided by the amine converts the hydroxyl group in the

105 carbinolamine into a much better leaving group (Figure 5). The barrier for the dehydration step

106 thereby decreases to 3.2–8.5 kcal·mol^{-1} for all anilines tested (Table 3). The operation of this

107 very favourable pathway depends, however, on the presence of extraneous acid to protonate the

108 base (aniline or toluidine), which calls into question its relevance for the elucidation of the

109 reaction mechanism in acid-free experimental conditions. On the other hand, the extremely high

110 reaction rates allowed by these low barriers ($4 \times 10^6 - 2.5 \times 10^{10}$ s^{-1}) entail that the experimental

111 reaction rates (on the order of 1 h^{-1}) can be achieved with minute concentrations of protonated

112 base ($10^{-14} - 10^{-12}$ mol·dm^{-3}). One so far over-looked source of such minute amounts of

113 protonated amine in acid-free conditions does exist: the auto-protolysis of the base, which would

114 generate one protonated (and one deprotonated) molecule of base from two neutral molecules of

115 base. Indeed, even some solvents generally regarded as aprotic or only weakly protic have been

116 shown to auto-ionize to a limited extent(Mihajlović et al., 1996). To ascertain the likelihood of

117 auto-protolysis of aniline and toluidines, we performed additional computations using small
118 clusters of amine molecules, one of which was kept protonated (or deprotonated). Since very
119 accurate results would require the simulation of very large solvent clusters to account for
120 possible long-range structural rearrangements around the ionized structures, which are
121 unfortunately not possible with our current computational resources, we compared our results
122 with the auto-protolysis constants, computed in the same way, of other solvents which have been
123 studied experimentally. Our results (Table 4) show that the auto-protolysis of all amines tested is
124 much more favourable than that of nitromethane (pKs=23.7) or acetonitrile (pKs=28.8), and that
125 therefore self-ionization of aniline or toluidines easily affords concentrations of protonated
126 amine at least as high as $10^{-23.7/2}$, in complete agreement with the hypothesis formulated above.

127

128 **Conclusions**

129

130 Like the analogous reaction in water (Ding, Cui & Li, 2015), imine formation from
131 benzaldehyde and anilines in apolar solvent cannot occur without the intervention of a
132 base which facilitates the transfer of one proton from the amine nitrogen atom to the
133 carbonyl oxygen. The energetic stabilization provided by this assistance decreases
134 activation energy by more than 10 kcal·mol^{-1} relative to the reaction in the gas phase,
135 enabling reasonable rates of formation of the carbinolamine. Dehydration of the
136 carbinolamine, in turn, is prohibitively expensive unless one proton source is available to
137 protonate the leaving hydroxyl group. Previous works assumed that protons would be
138 provided by added acids or water molecules and were therefore unable to explain the
139 occurrence of the reaction in the absence of acids or protic solvents. Our computations, in
140 turn, show that auto-protolysis of the amine is feasible and that the low activation
141 energies of the protonated amine-assisted dehydration of carbinolamine fully enable the
142 observation of good reaction rates from the very small concentrations of protonated amine
143 predicted to exist in water-free aniline/benzaldehyde mixtures.

144

145   **References**

146

147   Adamo C., Barone V. 1999. Toward reliable density functional methods without adjustable
148   parameters: The PBE0 model. *The Journal of Chemical Physics* 110:6158. DOI:
149   10.1063/1.478522.
150   Allen CFH., VanAllan J. 1941. m-tolylbenzylamine. *Organic Syntheses* 21:108. DOI:
151   10.15227/orgsyn.021.0108.
152   Amovilli C., Mennucci B. 1997. Self-consistent-field calculation of Pauli repulsion and
153   dispersion contributions to the solvation free energy in the polarizable continuum model.
154   *The Journal of Physical Chemistry B* 5647:1051–1057.
155   Baker J., Kessi A., Delley B. 1996. The generation and use of delocalized internal coordinates in
156   geometry optimization. *Journal of Chemical Physics* 105:192–212. DOI: 10.1063/1.471864.
157   Campbell KN., Helbing CH., Florkowski MP., Campbell BK. 1948. The Reaction of Grignard
158   Reagents with Schiff Bases. *Journal of the American Chemical Society* 70:3868–3870.
159   DOI: 10.1021/ja01191a099.
160   Ćmikiewicz A., Gordon AJ., Berski S. 2018. Characterisation of the reaction mechanism
161   between ammonia and formaldehyde from the topological analysis of ELF and catastrophe
162   theory perspective. *Structural Chemistry* 29:243–255. DOI: 10.1007/s11224-017-1024-x.
163   Cossi M., Mennucci B., Pitarch J., Tomasi J. 1998. Correction of cavity-induced errors in
164   polarization charges of continuum solvation models. *Journal of Computational Chemistry*
165   19:833–846. DOI: 10.1002/(sici)1096-987x(199806)19:8<833::aid-jcc3>3.0.co;2-q.
166   Crowell TI., Peck DW. 1953. Kinetic Evidence for a Schiff Base Intermediate in the
167   Knoevenagel Condensation. *Journal of the American Chemical Society* 75:1075–1077.
168   DOI: 10.1021/ja01101a018.
169   Ding YQ., Cui YZ., Li TD. 2015. New views on the reaction of primary amine and aldehyde
170   from DFT study. *Journal of Physical Chemistry A* 119:4252–4260. DOI:
171   10.1021/acs.jpca.5b02186.
172   Granovsky AA. PC GAMESS/Firefly version 7.1.G.
173   :http://classic.chem.msu.su/gran/gamess/index.html.
174   Grimme S., Antony J., Ehrlich S., Krieg H. 2010. A consistent and accurate ab initio
175   parametrization of density functional dispersion correction (DFT-D) for the 94 elements H-

176   Pu. *The Journal of chemical physics* 132:154104. DOI: 10.1063/1.3382344.

177   Hall NE., Smith BJ. 1998. High-Level ab Initio Molecular Orbital Calculations of Imine

178   Formation. *The Journal of Physical Chemistry A* 102:4930–4938. DOI: 10.1021/jp9810825.

179   Hammett LP. 1940. *Physical Organic Chemistry*. New York, N. Y.,: McGraw- Hill Book Co.,

180   Inc.

181   Jencks WP. 1959. Studies on the Mechanism of Oxime and Semicarbazone Formation. *Journal*

182   *of the American Chemical Society* 81:475–481. DOI: 10.1021/ja01511a053.

183   Jencks WP. 1964. *Mechanism and Catalysis of Simple Carbonyl Group Reactions*. Hoboken, NJ,

184   USA: John Wiley & Sons, Inc. DOI: 10.1002/9780470171813.

185   Jensen F. 2014. Unifying General and Segmented Contracted Basis Sets. Segmented Polarization

186   Consistent Basis Sets. *Journal of Chemical Theory and Computation* 10:1074–1085. DOI:

187   10.1021/ct401026a.

188   Law HD. 1912. XVII.—Electrolytic reduction. Part V. Benzylidene bases. *J. Chem. Soc., Trans.*

189   101:154–166. DOI: 10.1039/CT9120100154.

190   Mennucci B., Tomasi J. 1997. Continuum solvation models: A new approach to the problem of

191   solute's charge distribution and cavity boundaries. *Journal of Chemical Physics* 106:5151–

192   5158. DOI: 10.1063/1.473558.

193   Mihajlović R., Simić Z., Mihajlović L., Vukićević M. 1996. Determination of autoprotolysis

194   constants of some non-aqueous solvents using coulometric titration. *Talanta* 43:2131–2136.

195   DOI: 10.1016/S0039-9140(96)02000-0.

196   Santerre GM., Hansrote CJ., Crowell TI. 1958. The Reaction of Aromatic Aldehydes with n-

197   Butylamine. Acid Catalysis and Substituent Effects. *Journal of the American Chemical*

198   *Society* 80:1254–1257. DOI: 10.1021/ja01538a056.

199   Schmidt MW., Baldridge KK., Boatz JA., Elbert ST., Gordon MS., Jensen JH., Koseki S.,

200   Matsunaga N., Nguyen KA., Su S., Windus TL., Dupuis M., Montgomery JA. 1993.

201   General atomic and molecular electronic structure system. *Journal of Computational*

202   *Chemistry* 14:1347–1363. DOI: 10.1002/jcc.540141112.

203   Solís-Calero C., Ortega-Castro J., Hernàndez-Laguna A., Muñoz F. 2012. A comparative DFT

204   study of the Schiff base formation from acetaldehyde and butylamine, glycine and

205   phosphatidylethanolamine. *Theoretical Chemistry Accounts* 131:1–12. DOI:

206   10.1007/s00214-012-1263-2.

207   Tomasi J., Persico M. 1994. Molecular Interactions in Solution: An Overview of Methods Based

208   on Continuous Distributions of the Solvent. *Chemical Reviews* 94:2027–2094. DOI:
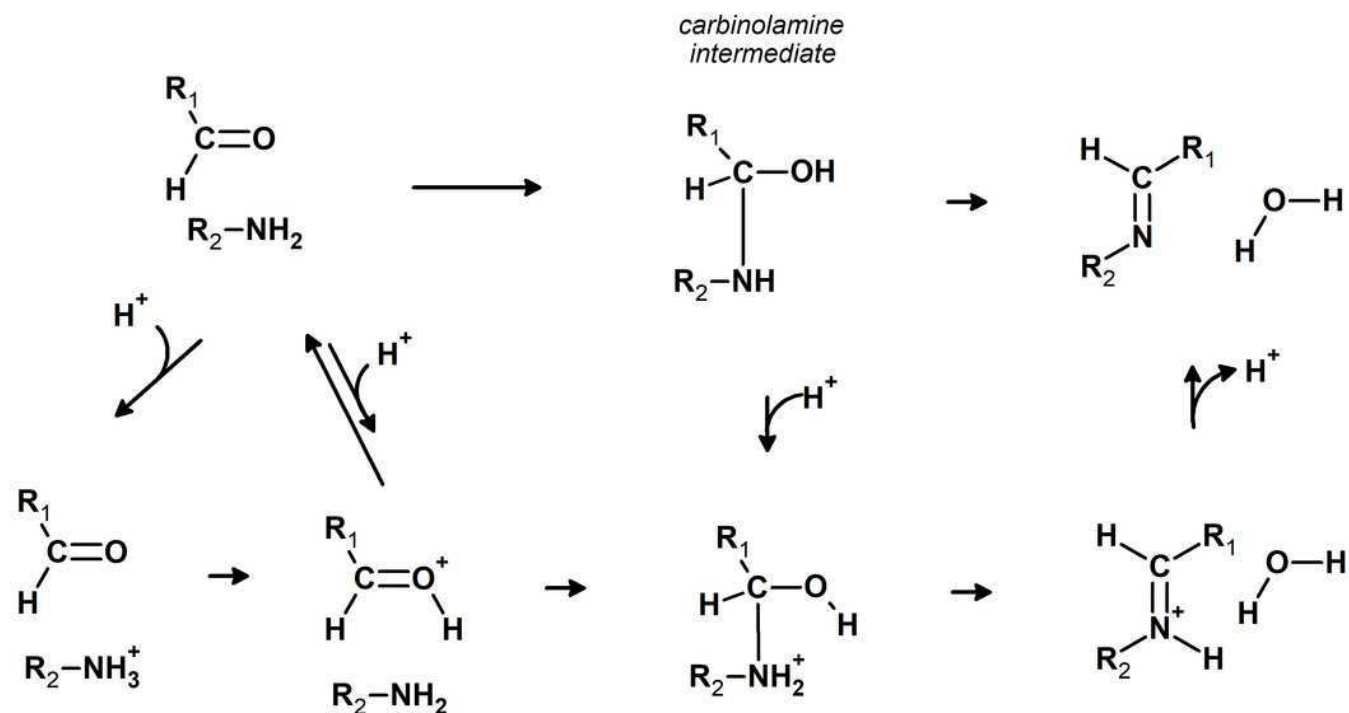
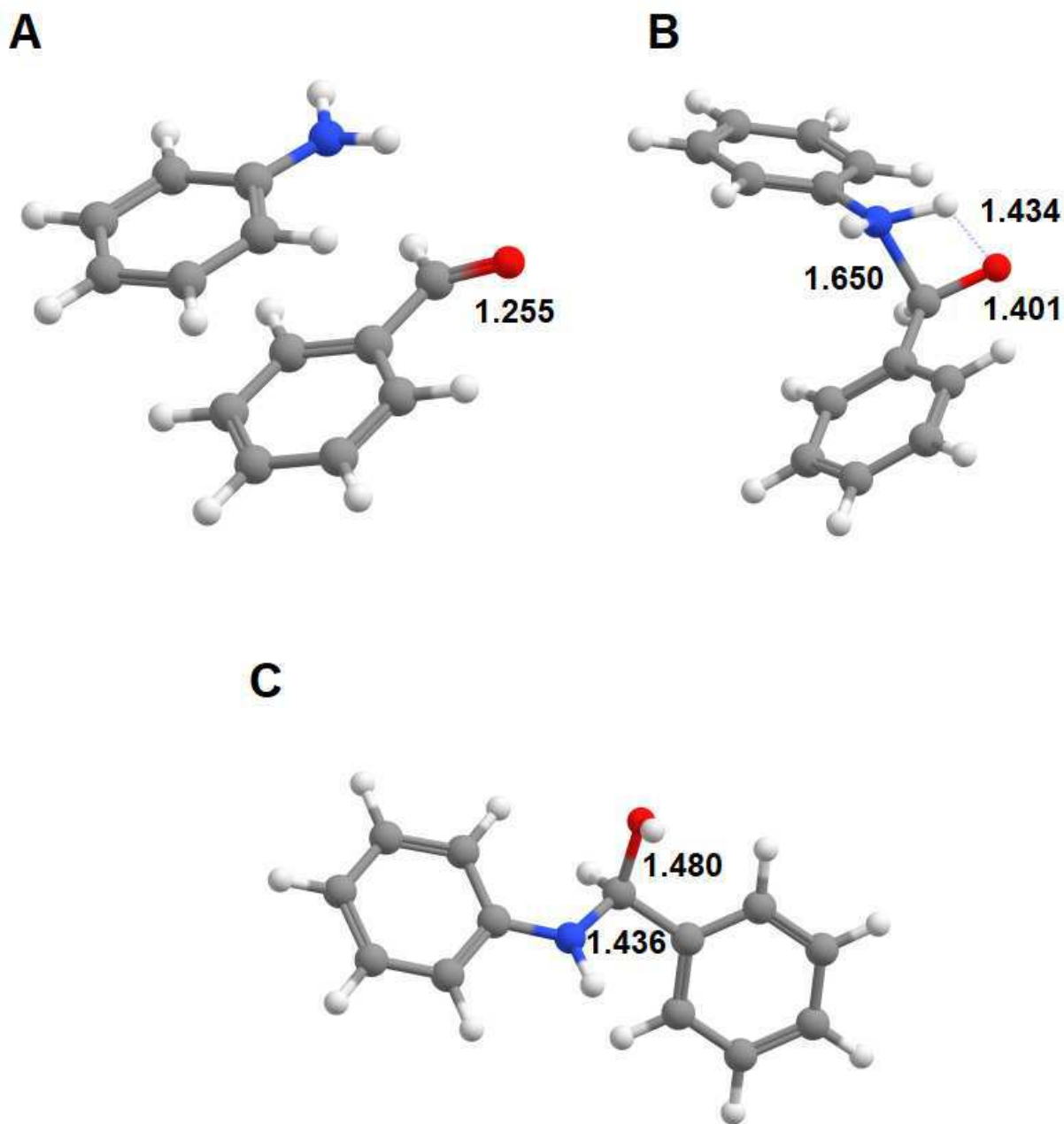209   10.1021/cr00031a013.

210

211

212

213

Figure 1

Possible pathways for the reaction of aldehydes with amines.

Figure 2

Structures of pre-reactional complex (A), transition state (B) and carbaminolamine (C) in the reaction between benzaldehyde and aniline.
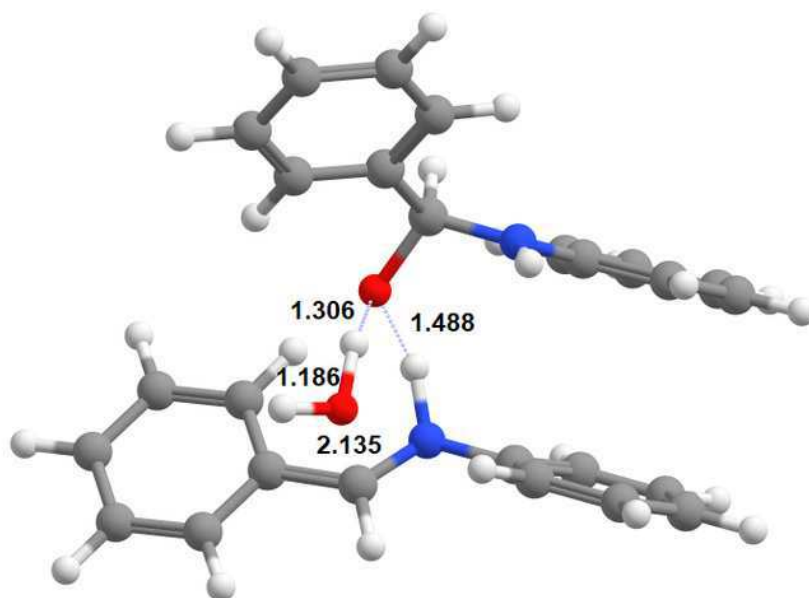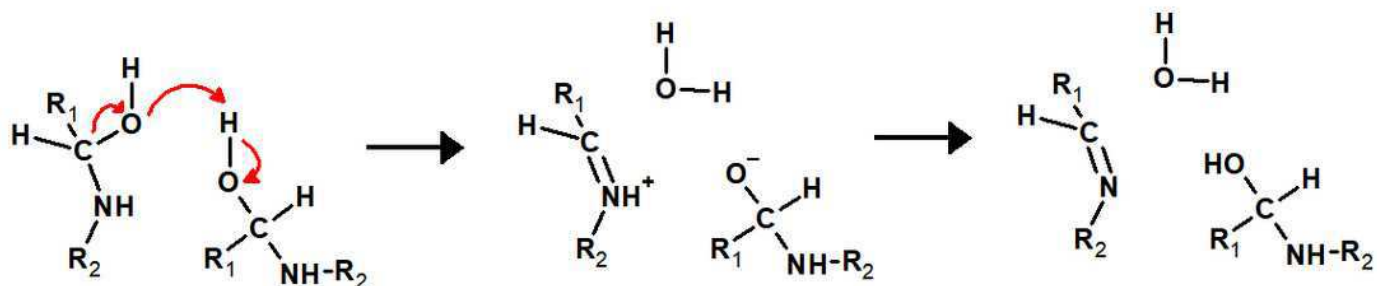
Figure 3

Structures of the transition state (A) , carbaminolamine (B) and dehydration transition state (C) of the aniline-assisted the reaction between benzaldehyde and aniline.
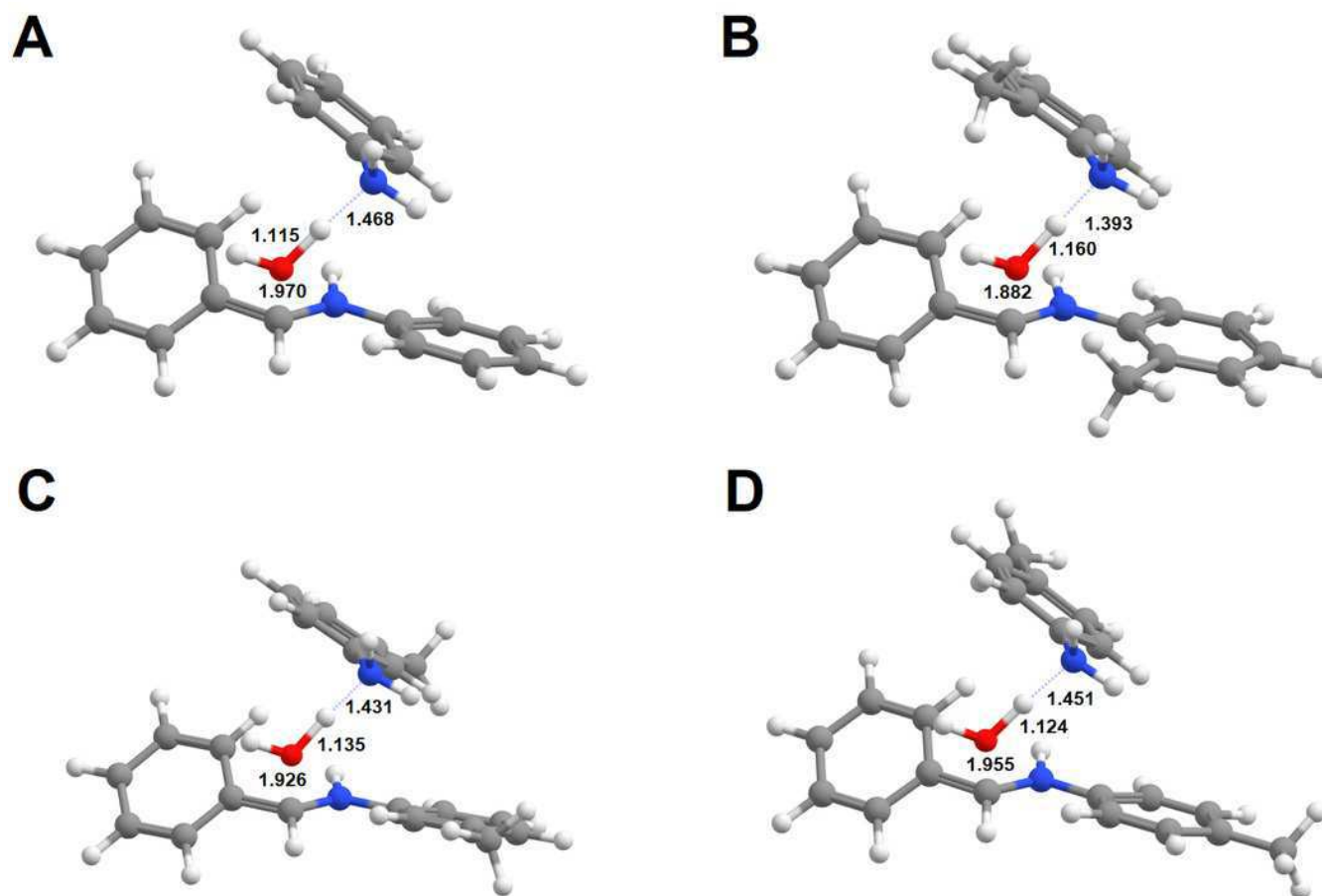
A

B

C
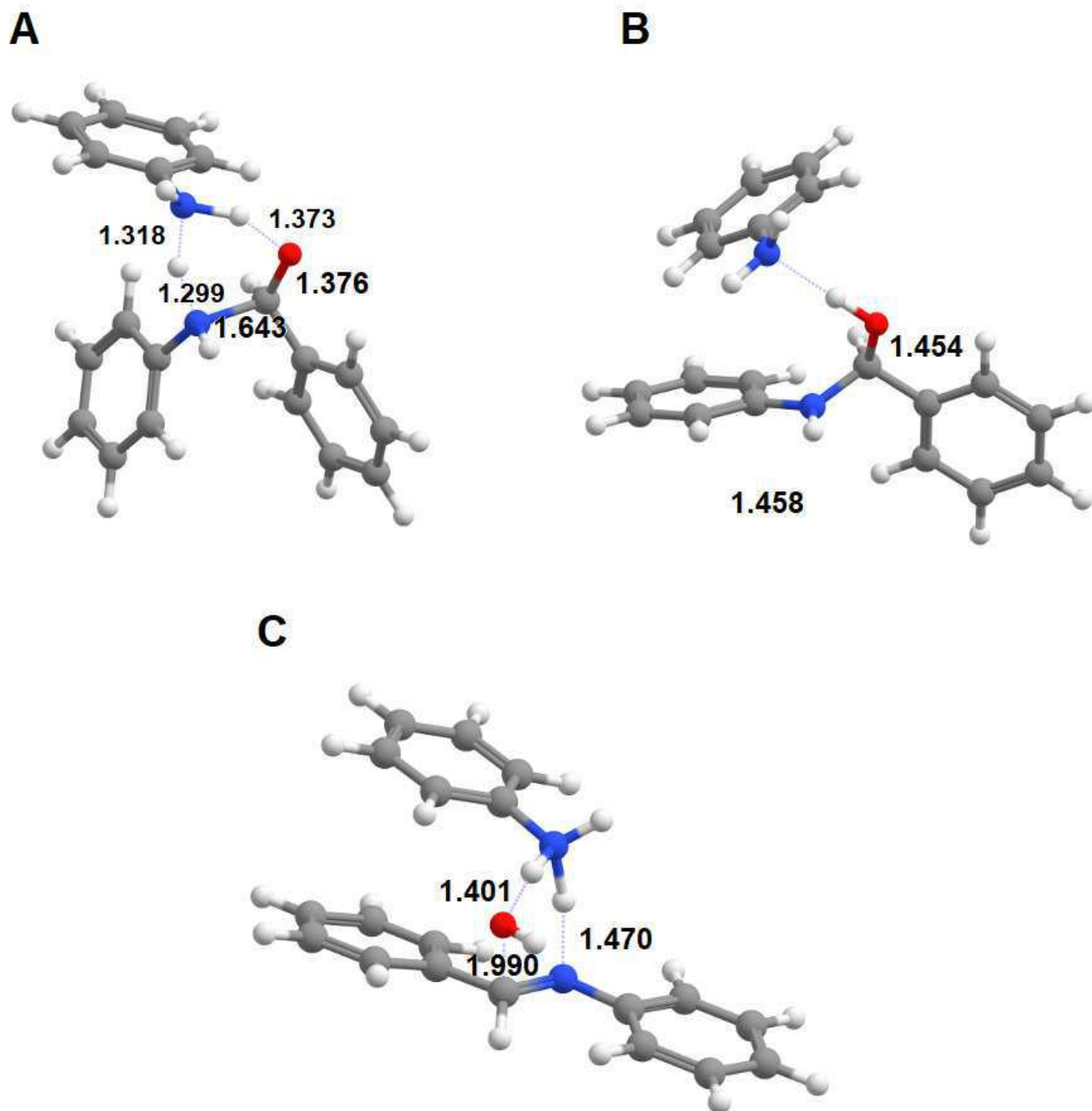
Figure 4

Proposed bimolecular carbaminolamine dehydration step, and respective transition state.

Figure 5

Transition states for the dehydration of the carbinolamines produced from aniline (A), *o*-toluidine (B), *m*-toluidine (C) and *p*-toluidine (D) in the presence of the protonated form of the amine.

Table 1(on next page)

Relative free energies (vs. infinitely separated reactants) of the species involved in the formation of carbinolamines from benzaldehyde and aniline derivatives

Computations performed at the PBE0-D3/(aug)-pcseg0//PBE0-D3/(aug)-pcseg2 theory level.

Solvation effects in toluene were included with the PCM formalism.

1 **Table 1: Relative free energies (vs. infinitely separated reactants) of the species involved in**

2 **the formation of carbinolamines from benzaldehyde and aniline derivatives, computed at**

3 **the PBE0-D3/(aug)-pcseg0//PBE0-D3/(aug)-pcseg2 theory level. Solvation effects in toluene**

4 **were included with the PCM formalism.**

	aniline	*o*-toluidine	*m*-toluidine	*p*-toluidine
pre-reactional complex	8.0	8.2	5.3	6.4
transition state	35.6	35.9	34.4	33.5
carbaminolamine	-0.2	-0.7	-0.4	-0.3

5

Table 2 (on next page)

Relative free energies (vs. infinitely separated reactants) of the species involved in the base-assisted formation of carbinolamines from benzaldehyde and aniline derivatives.

Computations performed at the PBE0-D3/(aug)-pcseg0//PBE0-D3/(aug)-pcseg2 theory level.

Solvation effects in toluene were included with the PCM formalism.

1 **Table 2: Relative free energies (vs. infinitely separated reactants) of the species involved in**

2 **the base-assisted formation of carbinolamines from benzaldehyde and aniline derivatives,**

3 **computed at the PBE0-D3/(aug)-pcseg0//PBE0-D3/(aug)-pcseg2 theory level. Solvation**

4 **effects in toluene were included with the PCM formalism.**

	aniline	*o*-toluidine	*m*-toluidine	*p*-toluidine
pre-reactional complex	12.0	7.6	6.2	7.2
transition state	24.8	21.8	19.1	20.7
carbaminolamine	8.7	4.4	2.6	7.6
dehydration transition state	35.7	35.5	34.7	34.4

5

Table 3(on next page)

Relative free energies (vs. infinitely separated reactants) of the species involved in the dehydration of carbinolamines assisted by the protonated forms of the respective bases.

Computations performed at the PBE0-D3/(aug)-pcseg0//PBE0-D3/(aug)-pcseg2 theory level.

Solvation effects in toluene were included with the PCM formalism.

1   **Table 3: Relative free energies (vs. infinitely separated reactants) of the species involved in**

2   **the dehydration of carbinolamines assisted by the protonated forms of the respective bases,**

3   **computed at the PBE0-D3/(aug)-pcseg0//PBE0-D3/(aug)-pcseg2 theory level. Solvation**

4   **effects in toluene were included with the PCM formalism.**

	aniline	*o*-toluidine	*m*-toluidine	*p*-toluidine
Carbaminolamine + protonated base	-0.7	7.5	0.8	-1.2
dehydration transition state	4.5	8.5	3.2	3.0
Protonated imine + H_2O + base	0.7	0.3	0.6	0.5

5

Table 4**(on next page)**

Estimated auto-protolysis energies (kcal·mol^{-1}) of different solvents.

Geometries optimized at the PBE0-D3/(aug)-pcseg0 level. Energies computed with PBE0-D3 with different basis sets. Solvation effects were included with the PCM formalism.

1 **Table 4: Estimated auto-protolysis energies (kcal·mol^{-1}) of different solvents. Geometries**

2 **optimized at the PBE0-D3/(aug)-pcseg0 level. Energies computed with PBE0-D3 with**

3 **different basis sets. Solvation effects were included with the PCM formalism.**

	(aug)-pcseg1	**pcseg1**	**pcseg2**
acetonitrile	49.6	54.6	48.5
nitromethane	52.2	59.4	49.1
aniline	32.4	35.0	38.0
m-toluidine	31.0	33.3	35.3
o-toluidine	34.1	35.8	38.7
p-toluidine	37.6	39.8	41.4

4